Tim → Jerry - This is a copy of a paper submitted to Applied surface science 14/08/03 2694

Thick Film Growth of High Optical Quality Low Loss (0.1dBcm^{-1}) Nd:$Gd_3Ga_5O_{12}$ on $Y_3Al_5O_{12}$ by Pulsed Laser Deposition

T. C. May-Smith, C. Grivas, D. P. Shepherd, R. W. Eason*

Optoelectronics Research Centre, University of Southampton

Highfield, Southampton, SO17 1BJ, UK

M. J. F. Healy

Ion Beam Analysis Facility, Cranfield University

RMCS Shrivenham, Swindon, Wiltshire, SN6 8LA, UK

Thick film growth of high optical quality Nd:$Gd_3Ga_5O_{12}$ (Nd:GGG) on $Y_3Al_5O_{12}$ (YAG) is reported, using the Pulsed Laser Deposition (PLD) technique. Nd:GGG films with thickness up to 135μm have been grown via sequential deposition runs and up to 40μm in a single deposition. X-ray diffraction analysis shows that epitaxial growth has occurred and also confirms that the thick Nd:GGG films are single crystal. Analysis by Rutherford backscattering spectrometry shows that the stoichiometry of the thick Nd:GGG films is close to that of bulk Nd:GGG. The thick Nd:GGG films have fluorescence and absorption properties similar to that of bulk Nd:GGG, but slightly broadened. The Findlay-Clay technique of loss calculation has yielded a value of 0.1dBcm^{-1} as an estimate of the propagation loss of one of the thick Nd:GGG films that we have subsequently used as a laser medium.

*Author for correspondence: Prof. R. W. Eason, Optoelectronics Research Centre, University of Southampton, Highfield, Southampton, SO17 1BJ, UK. Tel: +44 (0)2380 592 098. Fax: +44 (0)2380 593142. E-mail: rwe@orc.soton.ac.uk.

1. Introduction

Pulsed Laser Deposition (PLD) is well established as a technique for the growth of thin films of a wide range of materials [1]. PLD is often chosen as a fabrication method over rival thin film fabrication techniques because of the complications that multi-component materials with complex stoichiometries can introduce. Few thin film fabrication techniques are capable of preserving complex stoichiometries and maintaining high quality crystalline growth. Rival techniques suffer from a combination of low growth rates, the need for complex precursor chemicals or highly complicated experimental apparatus. These difficulties can be overcome however, and successful growth of $Y_3Al_5O_{12}$ (YAG) has been reported using metal-organic chemical vapour deposition (MOCVD) [2], growth of Nd:$Gd_3Ga_5O_{12}$ (Nd:GGG) and Nd:YAG has been reported using liquid phase epitaxy (LPE) [3-5] and the fabrication of Nd:YAG thin films has been reported using direct bonding [6,7]. Growth of thin optically waveguiding films of Nd:GGG and Nd:YAG by PLD has also been reported previously [8-15].

A well known problem with PLD grown optical waveguides is particulates [16], which arise in the fabrication process due to two main processes, incomplete vaporisation of the target material and exfoliation. Incomplete vaporisation of the target material is impossible to circumvent because it is an inherent consequence of the ablation process. Exfoliation is caused by overuse of the same spot on the target and can therefore be minimised by repositioning and re-polishing of the target. Particulates cause most problems when they are near or on the surface of optically waveguiding thin films, as the presence of such scattering centres can significantly contribute to the propagation loss. It has been shown previously that the effect of

particulates can be reduced by burial below the film surface [16]. The quality of the surface of optically waveguiding thin films becomes less critical when the guided modes exist further away from the surface, meaning thicker films will suffer less from the effect of surface particulates. Growth of thick films is also of interest as a first step towards multi-layer geometries for high power cladding pumped devices and it has been reported that thick films will be required for these devices to maximise the launch efficiency and absorption properties for high power diode pump sources [17].

In this paper, we report the use of PLD to grow *thick* Nd:GGG films for subsequent use as high power laser media. To our knowledge, this is the first report of PLD grown films of high quality crystalline materials with thickness > 100μm, at least an order of magnitude thicker than most previously reported PLD thin film growth. We report here growth of Nd:GGG films (grown on YAG substrates) with thickness up to 135μm that demonstrate high crystalline quality, correct stoichiometry and high optical quality. X-ray diffraction (XRD) results show that epitaxial Nd:GGG has been grown and confirm that it is also single crystal. Analysis by Rutherford backscattering spectrometry shows that the thick Nd:GGG films have a constant stoichiometry as a function of depth. Fluorescence and absorption properties of the thick Nd:GGG films are similar to that of bulk Nd:GGG, but slightly broadened due, we conclude, to a small gallium deficiency. The Findlay-Clay technique of loss calculation has yielded a value of $0.1 dBcm^{-1}$ as an estimate of the propagation loss of one of the thick Nd:GGG films that we have subsequently used as a laser medium.

2. Experimental Procedure

The experimental set-up used is shown in Figure 1. A 248nm KrF excimer laser (Lambda Physik, Germany) set to produce an output of 200mJ per pulse at 10Hz was used for ablation (pulse duration ~ 20ns); this resulted in an energy density of approximately $2Jcm^{-2}$ at the target surface. The target used was a single crystal bulk sample of 1%at Nd:GGG. The target was mounted on a rotating stage that changed direction of rotation with a period of one minute. A remotely controlled substrate-shutter was used to enable pre-deposition cleaning of the target surface by ablation without contaminating the substrate. All substrates were put through a micro-cleaning process before use to ensure contaminants were minimised. The substrates were mounted using ceramic alumina half cylinder pillars to minimise any heat sinking problems. The target surface to substrate distance used was 4.0cm.

********** Figure 1 **********

Substrate heating was performed with a raster scanned CO_2 laser (40W Synrad, USA) as reported previously [18]. This heating method is preferred because it provides homogeneous substrate heating without causing the entire chamber to heat up, which would increase desorption of contaminants from the chamber walls. An estimated substrate temperature of between 600 and 650°C was used when depositing. The ideal temperature for depositing was found by growing Nd:GGG films with different CO_2 laser output powers and subsequently comparing the XRD results.

The deposition chamber atmosphere was pumped down to below 5.0×10^{-3} Pa prior to deposition. Oxygen was introduced into the chamber and kept at a pressure of 2.0 ± 0.1 Pa whilst depositing. To remain at this pressure without the chamber atmosphere becoming stagnant, a two-stage vacuum pumping system

consisting of a Leybold turbo molecular vacuum pump (Turbovac TW 300) backed by a Leybold rotary vane vacuum pump (Trivac D8B) was used with an oil trap to prevent chamber contamination from backstreaming oil vapour. Extra air-cooling was used for the turbo molecular vacuum pump to prevent overheating.

Nd:GGG films with thickness up to 40μm were grown in a single deposition run. Nd:GGG films with thickness up to 135μm were also grown in multiple deposition runs. It was found that particulates and other defects increase significantly after two hours of continuous deposition, so when multiple deposition runs were carried out, individual deposition times of no more than one and a half hours were used. The target position was changed and/or re-polished between subsequent runs, as repeatability of all deposition conditions is crucial when performing sequential depositions. Once end-polished, any deviations from such identical growth conditions could easily be detected via the appearance of 'fault lines' separating the growth runs, indicating non-epitaxial growth.

Several steps were taken to increase the repeatability of chamber deposition conditions. Metal pipes with flanges were inserted into the chamber to prevent laser port windows from becoming coated during such long deposition times. The KrF excimer gases were refilled regularly to ensure consistent beam quality. The CO_2 laser was cooled with a water chilling system and the temperature of the chilling system was monitored throughout all depositions.

A Siemens D5000 X-ray diffractometer was used for XRD analysis of all the Nd:GGG films grown. A Tencor alpha step profiler was used to measure film thickness and an optical microscope was used to check for significant surface defects.

The backscattering analysis was conducted using 2.5 MeV helium and proton beams from the Cranfield University accelerator. Gadolinium to gallium ratios were

established from the energy spectra of backscattered helium ions, which easily resolve these elements from one another, but affords only insensitive oxygen analysis. Sensitive oxygen analysis was conducted by studying energy spectra of backscattered protons, which exhibit enhanced scattering from oxygen [19] but do not offer well resolved data for gadolinium and gallium.

Fluorescence spectra were recorded by launching an 808nm wavelength Ti:sapphire laser beam into the thick Nd:GGG films using a 5cm focal length lens for input coupling and a 10x objective lens for output coupling. An optical spectrum analyser (OSA) was used to collect and analyse the spectral emission from the waveguides. The absorption properties were found by measuring the transmitted output power from the waveguides as the Ti:sapphire laser wavelength was tuned between 790 and 830nm.

The same arrangement of pumping source and coupling lenses used for the fluorescence and absorption experiments was adopted for investigating the lasing performance at a wavelength of 1.06μm for a 40μm thick by 4.1mm long film. A laser cavity was formed by butt-coupling a high reflectivity (HR) input coupling mirror and output coupling mirrors with reflectivity values of HR, 1.5%, 2.5%, 4.5% and 12% to the end faces of the waveguide. The threshold for lasing using the above mentioned output coupling mirrors was subsequently measured for loss calculation via the Findlay-Clay technique [20].

3. Results and Discussion

XRD results show that the thick Nd:GGG films have good crystallinity and have grown in the expected epitaxial (100) orientation. Figure 2a shows an XRD spectrum of a 135μm thick Nd:GGG film. The peaks found from the XRD analysis represent the Nd:GGG (400) and (800) orientations, confirming that epitaxial growth has occurred on the YAG (100) substrates, and the absence of any other peaks confirms that the thick Nd:GGG films are fully oriented single crystal. Figure 2a includes an expanded view of the Nd:GGG (400) and (800) peaks so that the full width half maxima (FWHM) can be seen clearly. The FWHMs are 0.08 degrees and 0.11 degrees for the Nd:GGG (400) and (800) peaks respectively. A bare YAG substrate was analysed using XRD, and the FWHMs for the YAG (400) and (800) peaks were both measured as 0.06 degrees. The thick Nd:GGG film FWHMs compare well therefore with that of the bare YAG, from which we can conclude that the thick Nd:GGG films are of high crystal quality.

********** Figure 2a **********

We can also conclude from this XRD analysis that there is no deterioration in crystal structure as the films get thicker and more deposition runs are performed. The XRD spectrum of the 135μm thick Nd:GGG film is actually better than that of most of the thinner Nd:GGG films analysed. The reason for such good crystallinity far away from the substrate-film boundary may be due to the lattice relaxing after accommodating for the initial lattice mismatch of 2.9% at the substrate-film boundary.

Figure 2b shows an XRD spectrum with the Nd:GGG film and YAG substrate peaks in evidence (the YAG substrate peaks are observed because a small section of

bare YAG substrate was intentionally introduced into the X-ray beam path). The XRD peaks correspond to lattice d-spacing values of 3.09Å, 1.55Å, 2.98Å and 1.50Å (all to 3 sig. fig.) calculated from the Nd:GGG (400), Nd:GGG (800), YAG (400) and YAG (800) peaks respectively. These values agree to a very high precision with the Daresbury Inorganic Crystal Structure Database values of 3.096Å, 1.548 Å, 3.002Å and 1.501Å for the GGG (400), GGG (800), YAG (400) and YAG (800) peaks respectively [21]. The d-spacing values measured for the thick Nd:GGG films agree slightly less well with the database values for GGG than those of the measured YAG substrate values with the database values for YAG and we attribute this to the effect of the ~1at% Nd^{3+} doping on the film crystal lattice.

********** Figure 2b **********

Another way of determining if the correct phase of Nd:GGG has been grown is to compare the angular separations Δ[Nd:GGG (400) - YAG (400)] and Δ[Nd:GGG (800) - YAG (800)] of the XRD peaks. This is better than comparing to database values because all of the analysis can be performed under the same conditions and a comparison can be made to the target material, which is more relevant than comparing to undoped GGG. The Nd:GGG target was subjected to XRD analysis and the Nd:GGG (444) peak was measured as 51.20 degrees. Using trigonometry, values of 28.89 degrees and 59.86 degrees can be calculated from the Nd:GGG (444) peak for the expected values of the Nd:GGG (400) and (800) peaks respectively. The bare YAG substrate (400) and (800) peaks were measured as 29.95 degrees and 61.93 degrees respectively. We would therefore expect 1.06 degrees and 2.07 degrees between Nd:GGG and YAG for the (400) and (800) peak separations respectively. Our thick Nd:GGG films have values of 1.05 degrees and 2.27 degrees for the (400)

and (800) peak separations respectively, which is in good agreement with what we would expect.

Backscattering analysis was performed on a wedge-polished thick Nd:GGG film sample that was grown by multiple deposition runs, to determine the uniformity of the stoichiometry of the thick Nd:GGG film as a function of thickness. The sample used for backscattering analysis was wedge polished so that it was 0μm thick at one end and 31μm at the other end. Figures 3a and 3b respectively show the helium and proton backscattering spectra at seven points at 1mm intervals along the thick Nd:GGG film sample. The three leading edges in the spectra correspond to gadolinium, gallium and oxygen present at the surface, the edge heights give surface concentration and the plateau height below the energy of each edge gives shallow depth information. Gadolinium:Gallium ratios were derived from the top 0.2 microns of the exposed wedged surface whereas oxygen concentrations were derived over 3 microns due to the greater range of protons. The slight shift in energy of the front edges with increased thickness is consistent with surface charging of this electrically insulating sample. Figure 3c shows the Gd_3:Ga_X fraction and figure 3d shows the oxygen content in atomic percent calculated from the backscattering analysis as a function of distance along the thick Nd:GGG film.

********** Figure 3a **********

********** Figure 3b **********

********** Figure 3c **********

********** Figure 3d **********

The Gd_3:Ga_X fraction and the oxygen content are both consistent within the values of errors shown throughout the thick Nd:GGG film and multiple deposition run layers. If $x = 4.4$ is taken as an average value of the Gd_3:Ga_X fraction and 60% is

taken as an average value for the oxygen content in atomic percent, we can estimate an empirical formula of (Nd:)$Gd_3Ga_{4.4}O_{11.1}$ for the thick Nd:GGG film. There appears to be a slight positive trend in the Gd_3:Ga_X fraction results, which may indicate that the Nd:GGG film grows slightly more gallium deficient closer to the YAG substrate - Nd:GGG film boundary to accommodate for the lattice mismatch, and then the gallium content recovers as the lattice relaxes further away from the substrate.

Figure 4a and 4b show typical fluorescence spectra for the 1045 - 1080nm and 920 - 950nm spectral regions from one of the thick Nd:GGG films compared to a Nd:GGG film grown previously [9] and bulk Nd:GGG. The fluorescence spectra obtained from our thick Nd:GGG films appear slightly broadened; this is most likely due to small deficiencies in the crystal structure and stoichiometry as has already been detected from XRD and backscattering analysis. The thick Nd:GGG film fluorescence peaks in the 920 - 950nm region appear to be shifted from that of the bulk Nd:GGG spectrum by 1.2nm and 0.1nm respectively; this is also thought to be due to the slightly deficient crystal structure and stoichiometry. The positions of the peaks for our thick Nd:GGG film fluorescence spectrum around 1.06μm however are much closer to bulk than that of previously reported Nd:GGG film growth via PLD [9].

********** Figure 4a **********

********** Figure 4b **********

Figure 5 shows the absorption spectrum for the 790 - 830nm region of a thick Nd:GGG film compared to that of bulk Nd:GGG; the target was analysed with the same set-up as the film for direct comparison. Figure 5 is plotted in such a way that the absorption coefficient alpha can be read directly from the graph as a function of wavelength. The absorption coefficient at 808nm has been found to be typically $2.64cm^{-1}$ for the thick Nd:GGG films. This is significantly lower than the value of

4.53cm^{-1} at 808nm measured for the Nd:GGG target. From this we can conclude that the cross section and/or the Nd^{3+} concentration of the thick Nd:GGG films is different from that of the Nd:GGG target, as already suggested from the results of the XRD and backscattering analysis. It is also likely that some Nd^{3+} may have been lost in the deposition process, an effect we have also observed for previous depositions including dopants of Nd^{3+} and Ti^{3+} [22].

********** Figure 5 **********

Figure 6 shows the results of the Findlay-Clay loss experiment. The absorbed power threshold is plotted on the y-axis against the natural logarithm of output coupler reflectivity R divided by the round trip cavity length 2L on the x-axis. This allows the propagation loss coefficient to be read directly from the graph as the x-axis intercept when y = 0 for the best fit line through the data points. Conversion to units of dBcm^{-1} yields a value of 0.1dBcm^{-1} as an estimate of the propagation loss, a value that approaches that of bulk garnet crystals, which is reported to be $\approx$ 0.03dBcm^{-1} [23], and is the lowest loss reported to date for a PLD grown waveguide to the best of our knowledge. The error values were estimated from the fluctuations in the power meter readings. These results will be further discussed in the context of our recent lasing experiments using the thick Nd:GGG films to be reported in a separate submission [24].

********** Figure 6 **********

From all of these results, we can conclude that the use of multiple PLD deposition runs is a good way of producing thick films that retain the same high quality as thin films. As long as care is taken to ensure identical deposition conditions are used in each run, different layers grow epitaxially as if the deposition was continuous.

4. Conclusion

We have successfully grown thick epitaxial single crystal Nd:GGG (100) with thickness up to 135μm on YAG (100) substrates with a view to decreasing the affect of particulates on propagation loss, and as a first step towards the fabrication of multi-layer thick waveguides suitable for high power cladding pumping. Growth in multiple deposition runs has been shown to be possible using PLD without suffering any significant loss in film quality as the thickness increases. We have shown that thick Nd:GGG films grown by PLD can have losses approaching that of bulk garnet crystals, which is reported to be $\approx 0.03 dBcm^{-1}$.

Acknowledgements

The authors would like to acknowledge the support of the Engineering and Physical Sciences Research Council (EPSRC) for funding under Grant No. GR/R74154/01. The authors would also like to acknowledge the services of the EPSRC National Crystallography Service based in the Chemical Crystallography Laboratory at the Department of Chemistry, University of Southampton. One of the authors (T. C. May-Smith) also acknowledges the receipt of an EPSRC studentship.

References

[1] D. B. Chrisey, G. K. Hubler, Pulsed Laser Deposition of Thin Films, Wiley, New York, (1994).

[2] G. R. Bai, H. Zhang, H. L. M Chang, C. M. Foster, Appl. Phys. Lett. **64** (14) 1777 (1994).

[3] B. Ferrand, D. Pelenc, I. Chartier, C. Wyon, J. Cryst. Growth. **128** (1-4) 966 (1993).

[4] C. L. Bonner, C. T. A. Bonner, D. P. Shepherd, W. A. Clarkson, A. C. Tropper, D. C. Hanna, B. Ferrand, Opt. Lett. **23** (12) 942 (1998).

[5] R. Gerhardt, J. Kleine-Börger, L. Beilschmidt, M. Frommeyer, H. Dötsch, B. Gather, Appl. Phys. Lett. **75** (9) 1210 (1999).

[6] D. P. Shepherd, C. L. Bonner, C. T. A. Brown, W. A. Clarkson, A. C. Tropper, D. C. Hanna, H. E. Meissner, Opt. Comm. **160** (1-3) 47 (1999).

[7] C. T. A. Brown, C. L. Bonner, T. J. Warburton, D. P. Shepherd, A. C. Tropper, D. C. Hanna, Appl. Phys. Lett. **71** (9) 1139 (1997).

[8] N. A. Vainos, C. Grivas, C. Fotakis, R. W. Eason, A. A. Anderson, D. S. Gill, D. P. Shepherd, M. Jelinek, J. Lancok, J. Sonsky, Appl. Surf. Sci, **127-129** 514 (1998).

[9] A. A. Anderson, C. L. Bonner, D. P. Shepherd, R. W. Eason, C. Grivas, D. S. Gill, N. Vainos, Opt. Commun. **144** (4-6) 183 (1997).

[10] C. L. Bonner, A. A. Anderson, R. W. Eason, D. P. Shepherd, D. S. Gill, C. Grivas, N. Vainos, Opt. Lett. **22** (13) 988 (1997).

[11] D. S. Gill, A. A. Anderson, R. W. Eason, T. J. Warburton, D. P. Shepherd, Appl. Phys. Lett. **69** (1) 10 (1996).

[12] S. Fukaya, T. Hasegawa, Y. Ishida, T. Shimoda, M. Obara, Appl. Surf. Sci. **177** (3) 147 (2001).

[13] H. Kumagai, K. Adachi, M. Ezaki, K. Toyoda, M. Obara, Appl. Surf. Sci. **109/110** 528 (1997).

[14] M. Ezaki, M. Obara, H. Kumagai, K. Toyoda, Appl. Phys. Lett. **69** (20) 2977 (1996).

[15] M. Ezaki, H. Kumagai, K. Kobayashi, K. Toyoda, M. Obara, Jpn. J. Appl. Phys. Part 1 – Regul. Pap. Short Notes Rev. Pap. **34** (12B) 6838 (1995).

[16] S. J. Barrington, T. Bhutta, D. P. Shepherd, R. W. Eason, Opt. Commun. **185** (1-3) 145 (2000).

[17] D. P. Shepherd, S. J. Hettrick, C. Li, J. I. Mackenzie, R. J. Beach, S. C. Mitchell, H. E. Meissner, J. Phys. D-Appl. Phys. **34** (16) 2420 (2001).

[18] S. J. Barrington, R. W. Eason, Rev. Sci. Instrum. **71** (11) 4223 (2000).

[19] A. F. Gurbich. Nucl. Instr. & Meth. B **129** p311 (1997).

[20] D. Findlay, R. A. Clay. Phys. Lett. **20** p277 (1966).

[21] Inorganic Crystal Structure Database (ICSD), part of the Chemical Database Service (CDS) based at Daresbury Laboratory UK. http://cds3.dl.ac.uk/dif/icsd/

[22] A. A. Anderson, R. W. Eason, M Jelinek, C. Grivas, D. Lane, K. Rogers, L. M. B. Hickey, C. Fotakis. Thin Solid Films, **300** (1-2) p68 (1997).

[23] T. Nishimura, T. Omi. Jpn. J. Appl. Phys. **14** p1011 (1975).

[24] C. Grivas, T. C. May-Smith, D. P. Shepherd, R. W. Eason. Opt. Commun. Submitted August 2003.

Figure Captions

Figure 1 PLD chamber apparatus.

Figure 2a 135μm thick Nd:GGG film XRD spectrum.

Figure 2b Typical thick Nd:GGG film XRD spectrum with YAG substrate in evidence.

Figure 3a Helium ion backscattering spectrum. Legend shows the distance along the sample at which analysis was performed for each data series. (3mm position corresponds to ~3μm thickness, 9mm position corresponds to ~27μm thickness).

Figure 3b Proton backscattering spectrum. Legend shows the distance along the sample at which analysis was performed for each data series. (3mm position corresponds to ~3μm thickness, 9mm position corresponds to ~27μm thickness). (data not shown for energies below 1500keV and 1000keV for the 3mm and 4mm positions respectively due to interference from the YAG substrate).

Figure 3c Gd_3:Ga_X fraction derived from helium ion backscattering spectrum.

Figure 3d Oxygen at% content derived from proton backscattering spectrum.

Figure 4a Typical thick Nd:GGG film fluorescence spectrum of 1045 - 1080nm region compared to that of bulk Nd:GGG and a previously reported thin Nd:GGG film [9]. Graph is normalised to 'area under curve'.

Figure 4b	Typical film fluorescence spectrum of 920 - 950nm region compared to that of bulk Nd:GGG. Graph is normalised to 'area under curve'.
Figure 5	Thick Nd:GGG film absorption spectrum compared to that of bulk Nd:GGG for 790 - 830nm region.
Figure 6	Findlay-Clay loss experiment results.

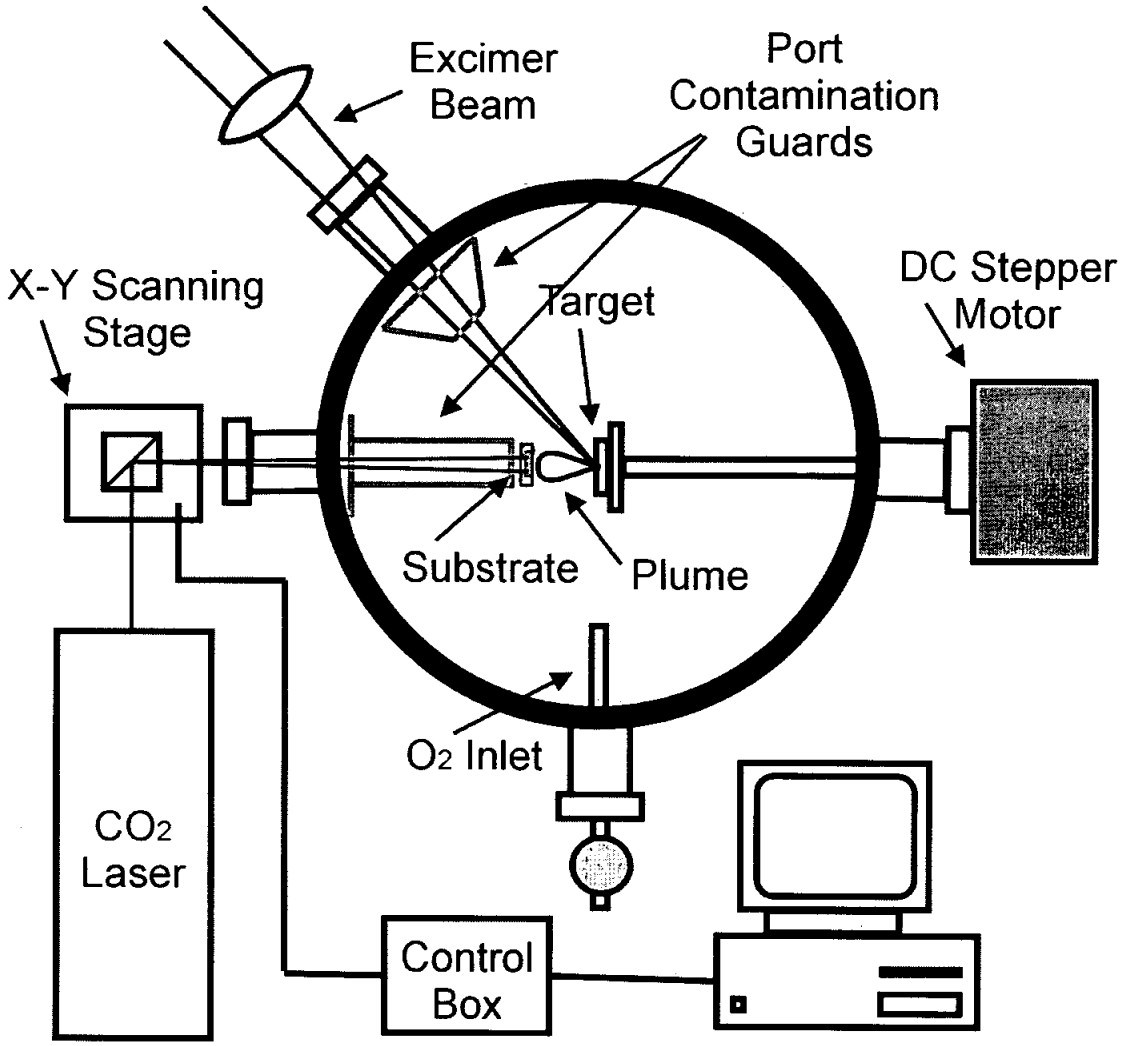
Excimer
Beam
Port
Contamination
Guards
X-Y Scanning
Stage
Target
DC Stepper
Motor
Substrate
Plume
O2 Inlet
CO2
Laser
Control
Box

Figure 1

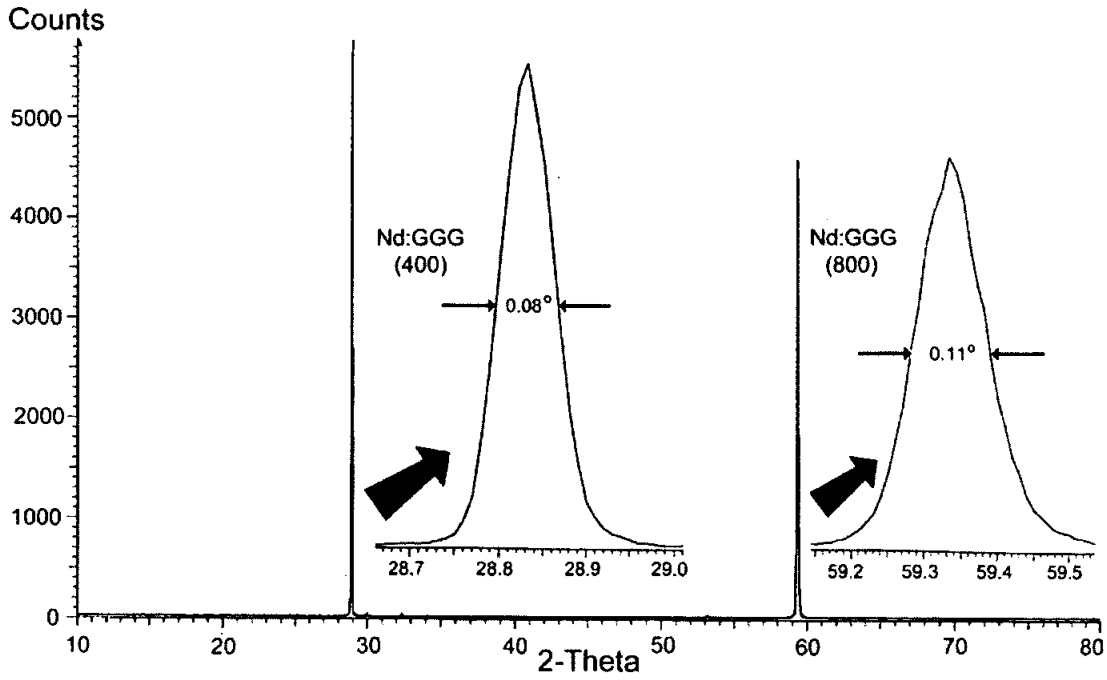
Counts
5000
4000
3000
2000
1000
0
10
20
30
40
50
60
70
80
2-Theta
Nd:GGG
(400)
0.08°
28.7
28.8
28.9
29.0
Nd:GGG
(800)
0.11°
59.2
59.3
59.4
59.5

Figure 2a

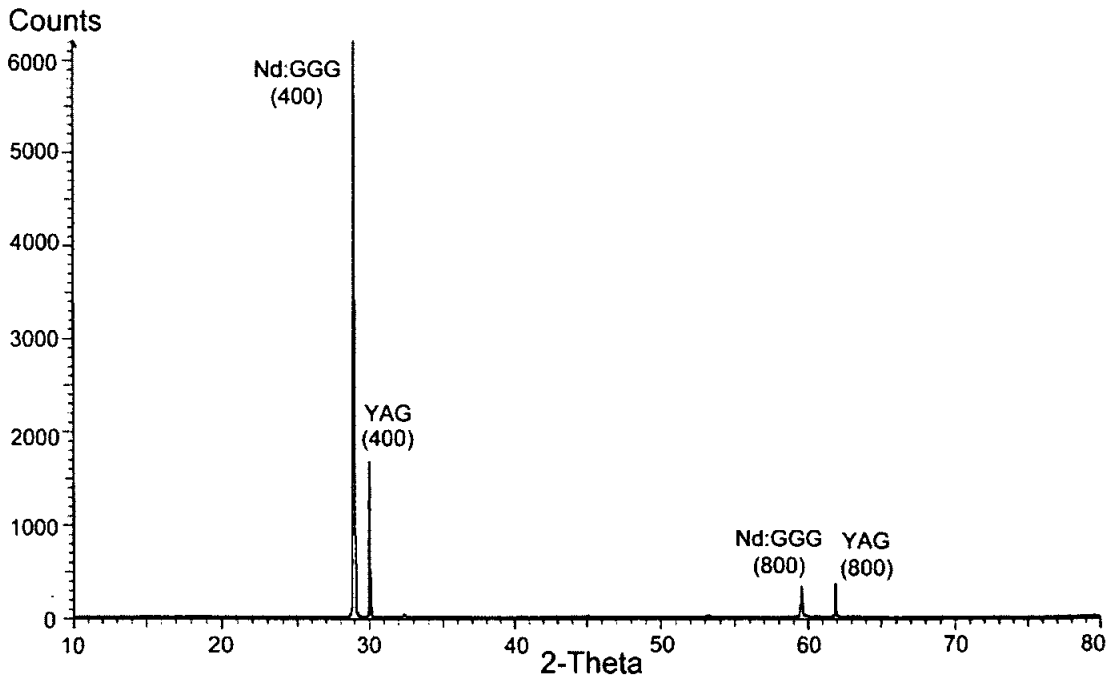
Counts
6000
5000
4000
3000
2000
1000
0
Nd:GGG
(400)
YAG
(400)
Nd:GGG
(800)
YAG
(800)
10
20
30
40
50
60
70
80
2-Theta

Figure 2b

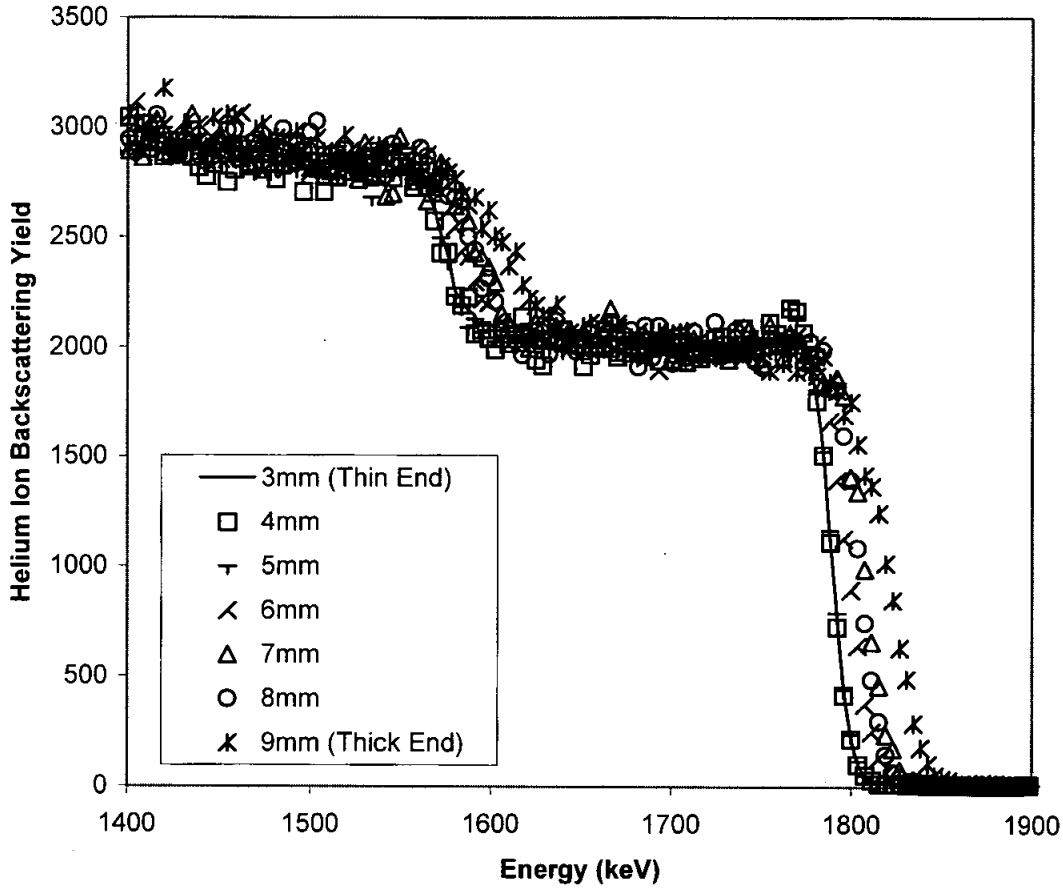
Helium Ion Backscattering Yield
Energy (keV)
3500
3000
2500
2000
1500
1000
500
0
1400
1500
1600
1700
1800
1900
3mm (Thin End)
4mm
5mm
6mm
7mm
8mm
9mm (Thick End)

Figure 3a

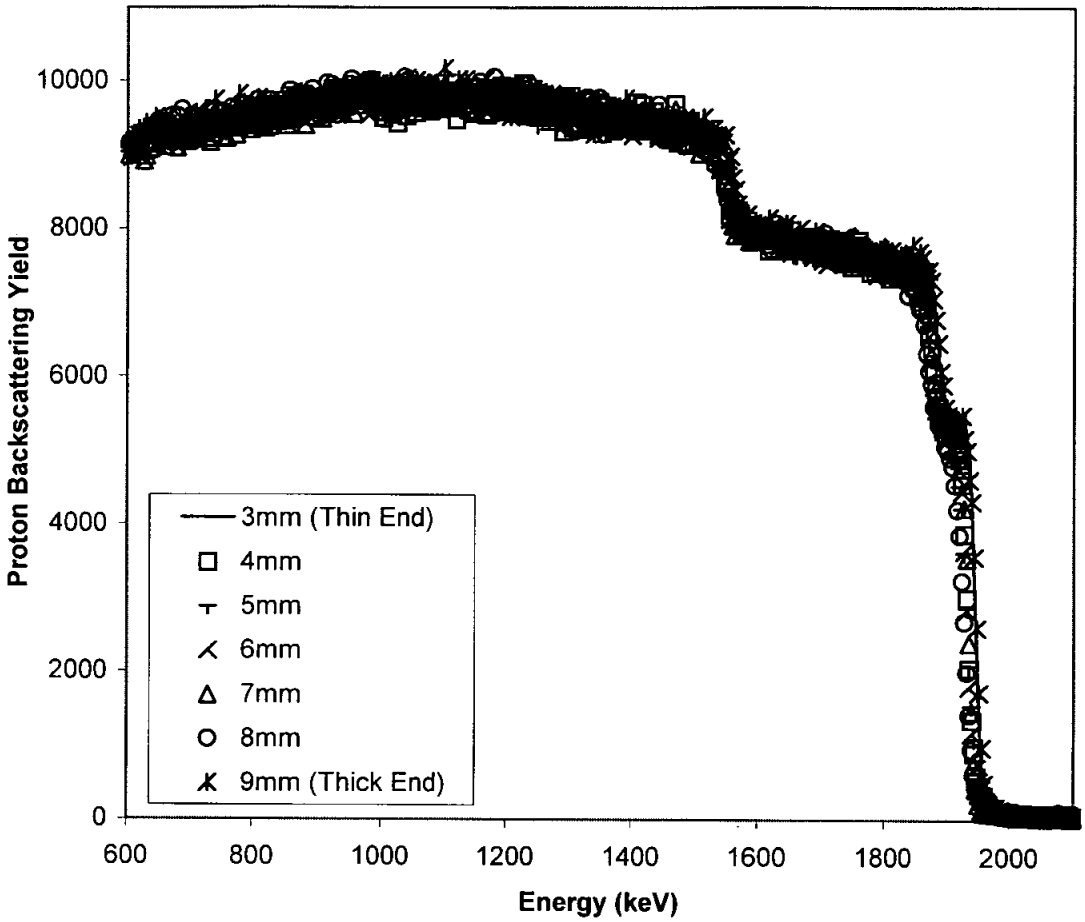
Proton Backscattering Yield
10000
8000
6000
4000
2000
0
600
800
1000
1200
1400
1600
1800
2000
Energy (keV)
3mm (Thin End)
4mm
5mm
6mm
7mm
8mm
9mm (Thick End)

Figure 3b

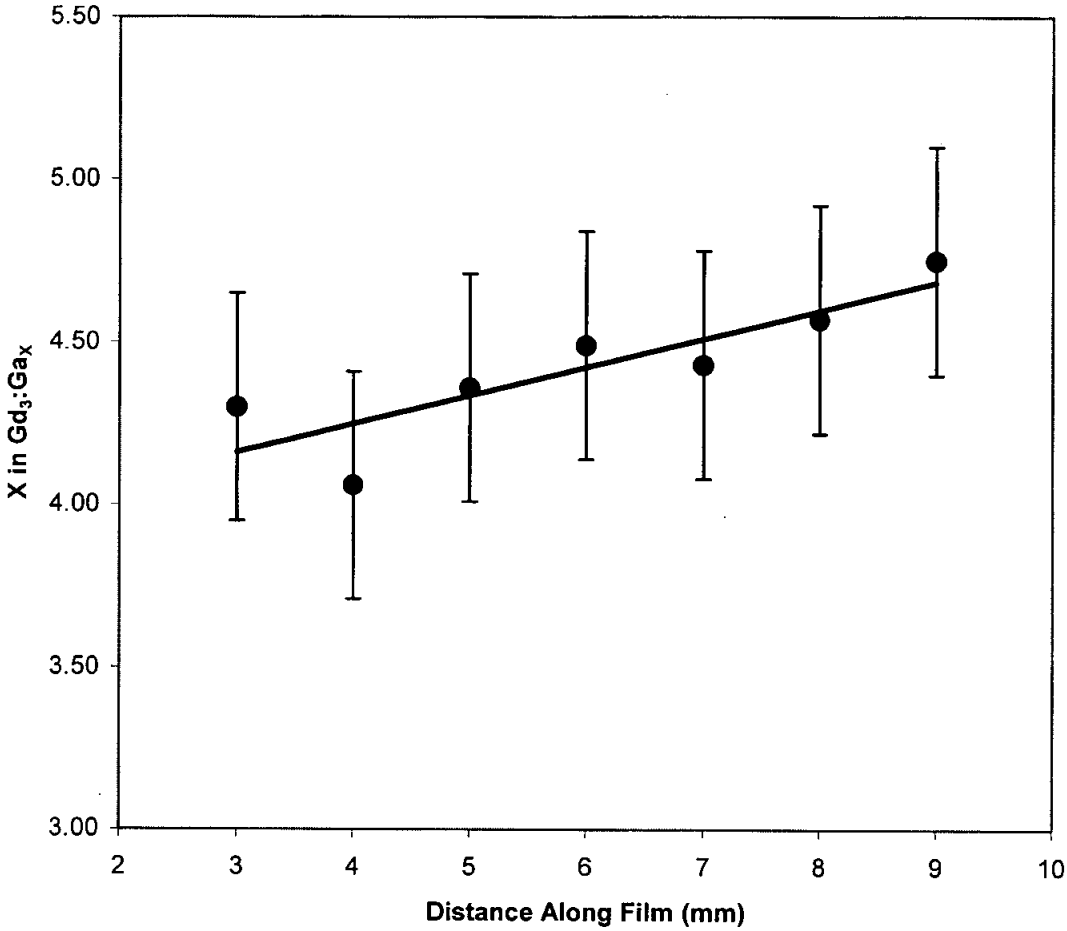
5.50
5.00
4.50
4.00
3.50
3.00
X in Gd3:GaX
2
3
4
5
6
7
8
9
10
Distance Along Film (mm)

Figure 3c

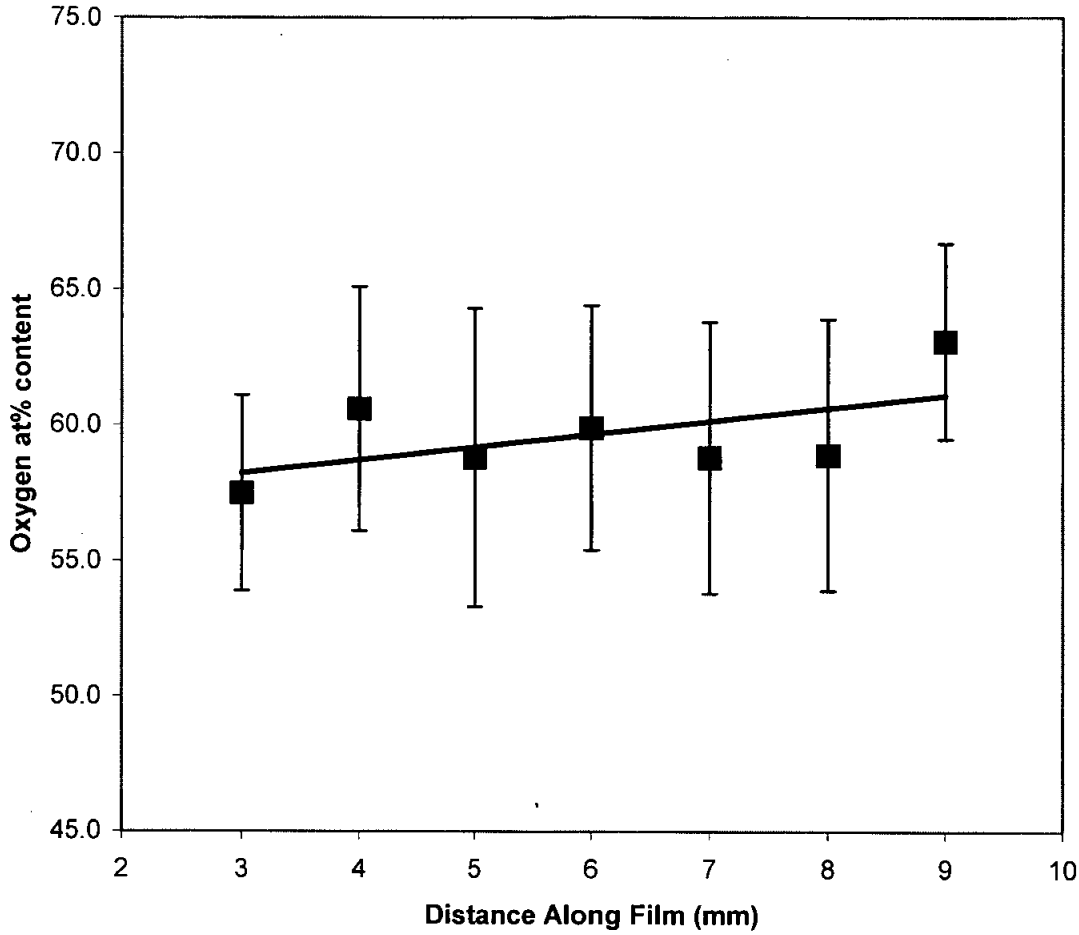
75.0
70.0
65.0
60.0
55.0
50.0
45.0
Oxygen at% content
2
3
4
5
6
7
8
9
10
Distance Along Film (mm)

Figure 3d

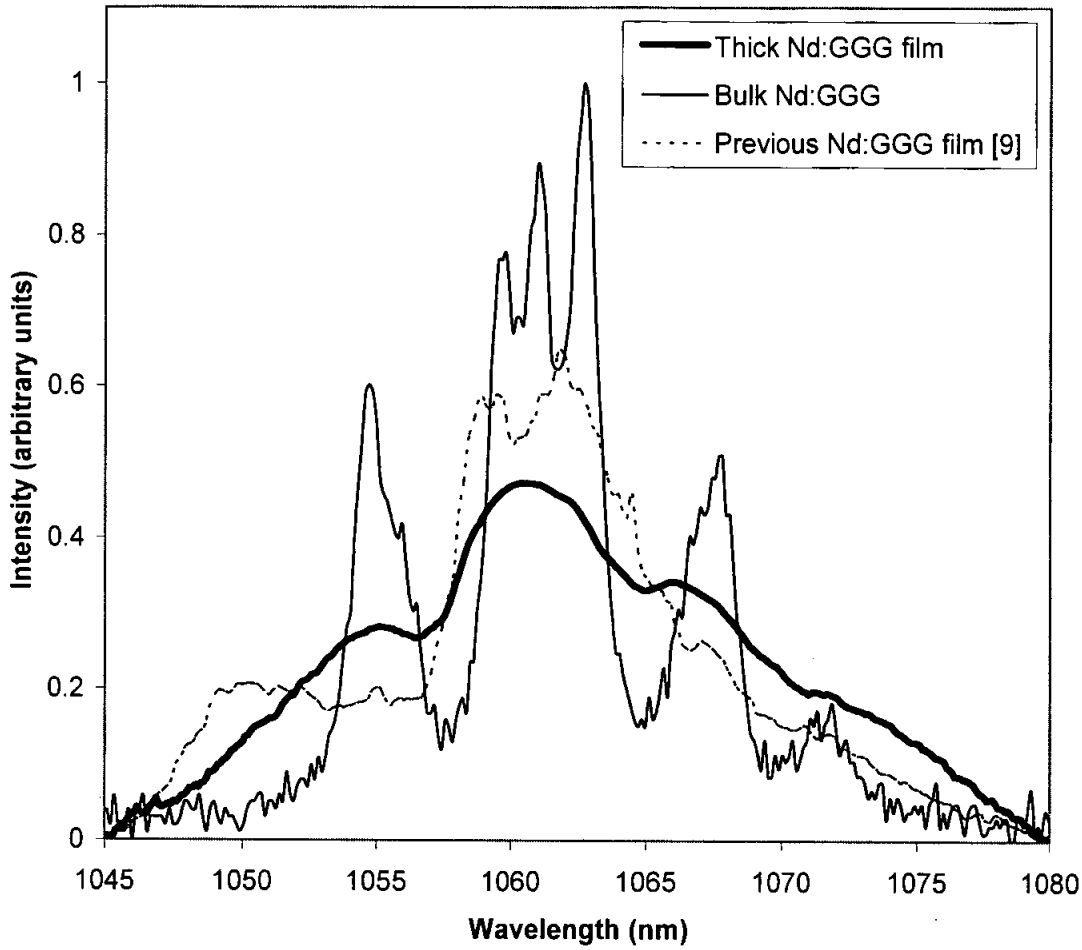
Thick Nd:GGG film
Bulk Nd:GGG
Previous Nd:GGG film [9]
Intensity (arbitrary units)
0
0.2
0.4
0.6
0.8
1
1045
1050
1055
1060
1065
1070
1075
1080
Wavelength (nm)

Figure 4a

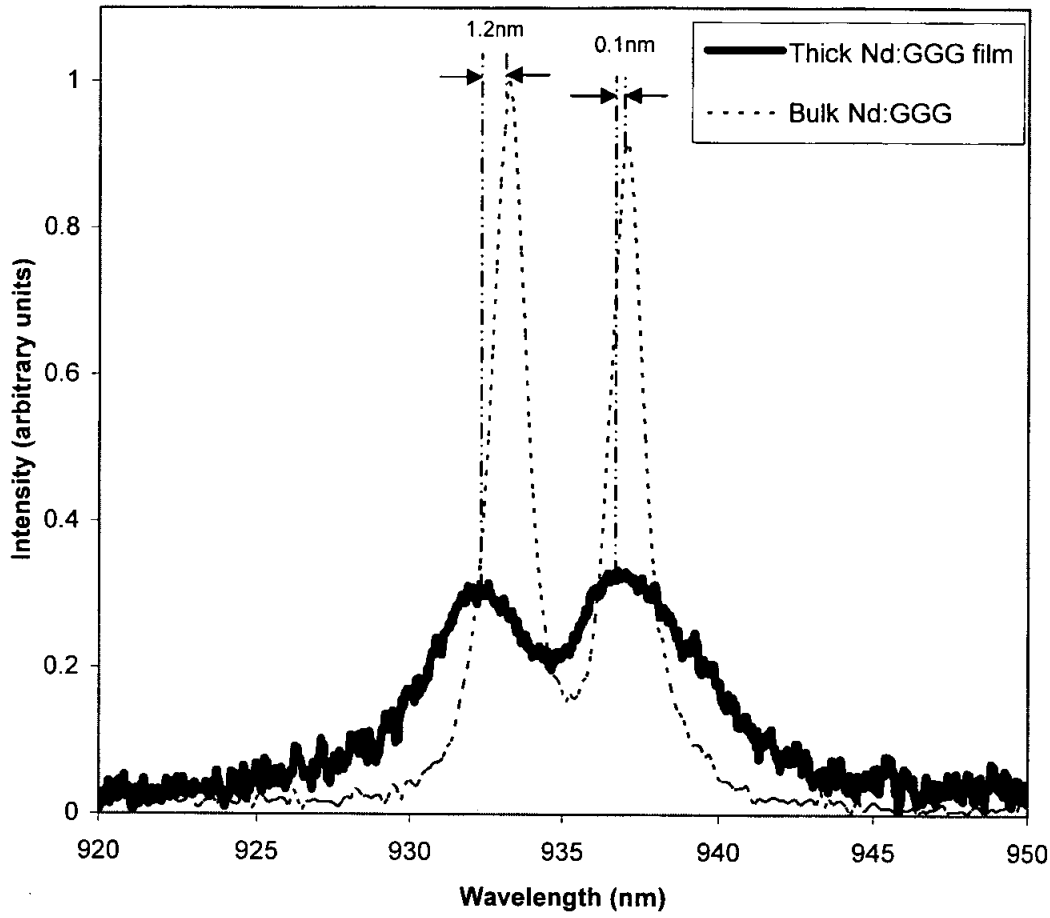
1.2nm
0.1nm
Thick Nd:GGG film
Bulk Nd:GGG
Intensity (arbitrary units)
0
0.2
0.4
0.6
0.8
1
920
925
930
935
940
945
950
Wavelength (nm)

Figure 4b

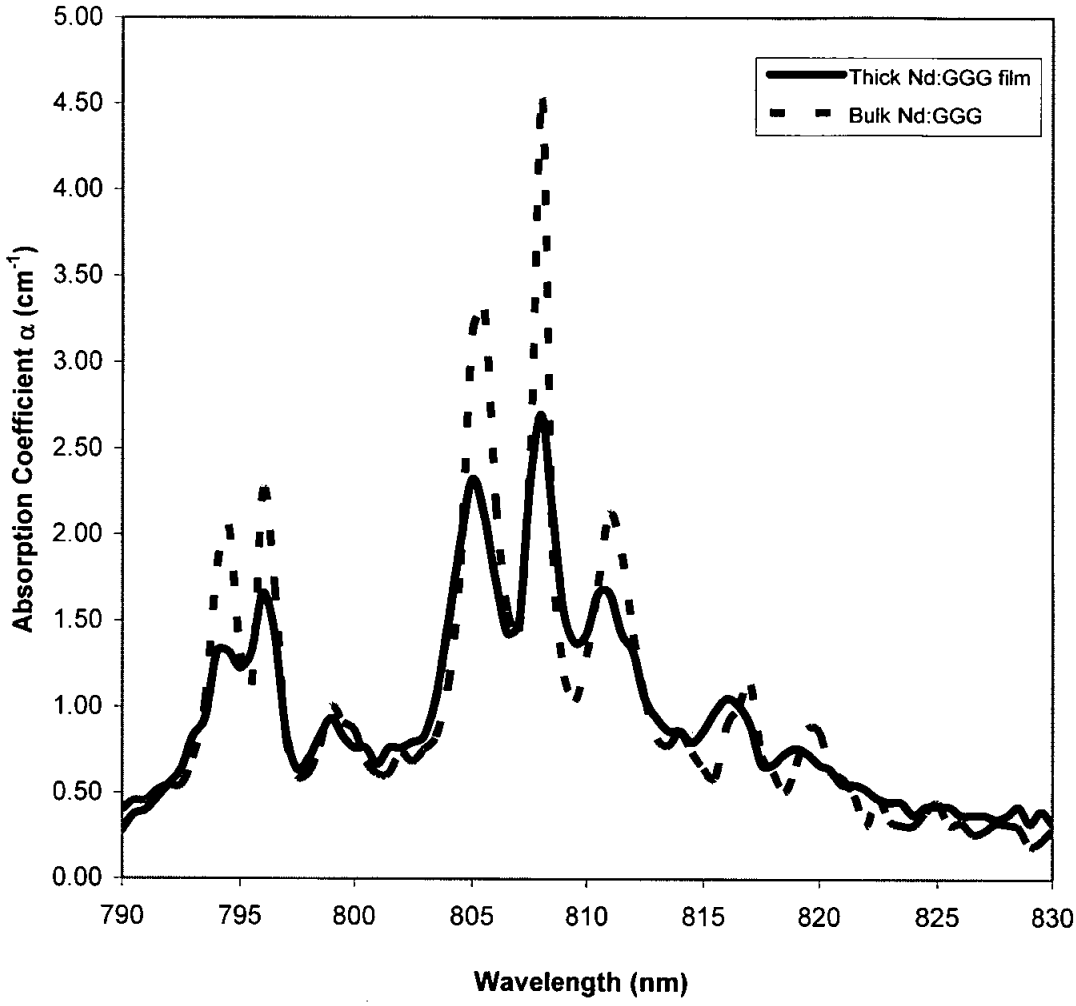
Thick Nd:GGG film
Bulk Nd:GGG
Absorption Coefficient α (cm-1)
Wavelength (nm)
5.00
4.50
4.00
3.50
3.00
2.50
2.00
1.50
1.00
0.50
0.00
790
795
800
805
810
815
820
825
830

Figure 5

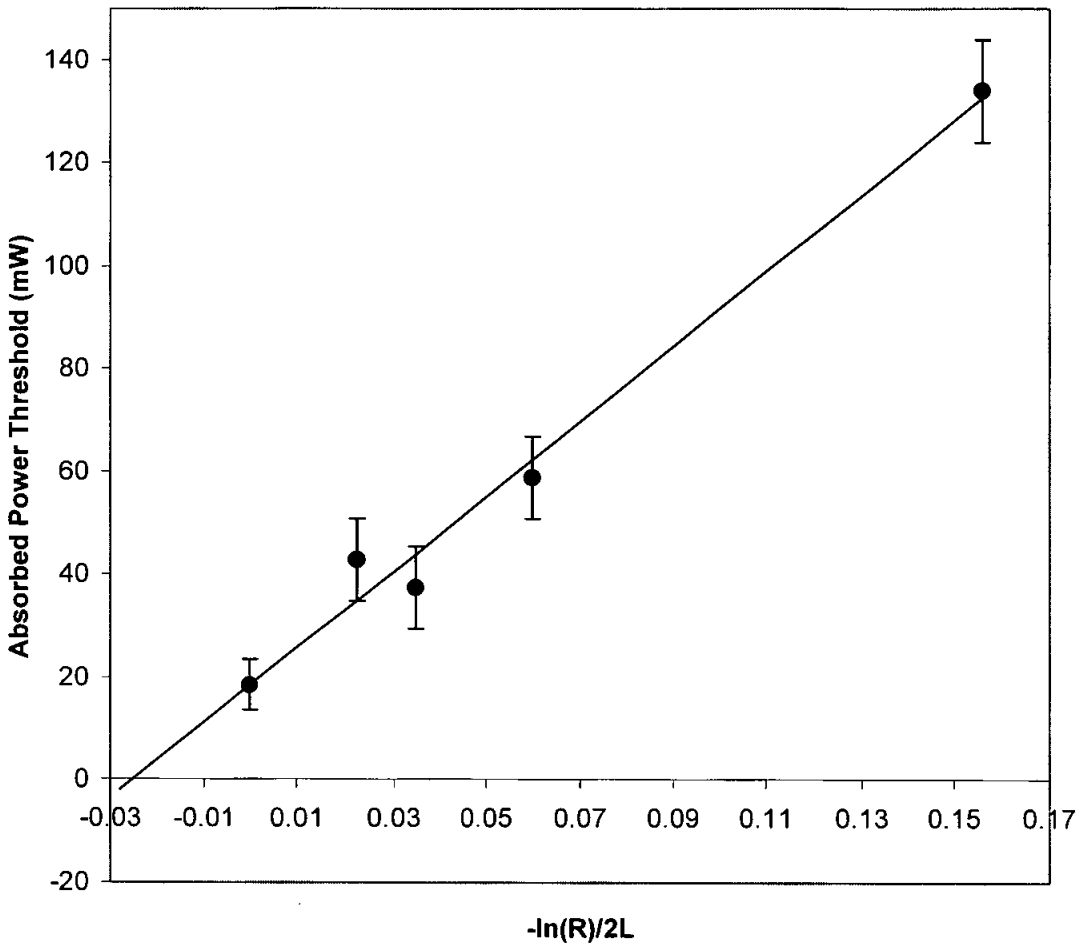
Absorbed Power Threshold (mW)
140
120
100
80
60
40
20
0
-20
-0.03
-0.01
0.01
0.03
0.05
0.07
0.09
0.11
0.13
0.15
0.17
-ln(R)/2L

Figure 6

PACS: 78.66.-w

81.15.Fg

42.70.Hj

42.55.Xi

Keywords: Nd:GGG

Pulsed Laser Deposition

Garnet Crystal

Optical

Waveguide

Film